

## Synthesis of Zinc Oxide/Reduced Graphene Oxide Composites for Fabrication of Anodes in Dye-Sensitized Solar Cells

Tran Trung Nghia Le<sup>a</sup>, Van Cuong Le<sup>a</sup>, Tien Phat Le<sup>b</sup>, Thi Tra My Nguyen<sup>b</sup>, Huu Dat Ho<sup>b</sup>, Khac Hung Le<sup>b</sup>, Minh Hien Tran<sup>c</sup>, Thai Hoang Nguyen<sup>c</sup>, Trong Liem Chau Pham<sup>a</sup>, Hoang Minh Nam<sup>a</sup>, Mai Thanh Phong<sup>b</sup>, Nguyen Huu Hieu<sup>a,\*</sup>

<sup>a</sup>VNU-HCM Key Laboratory of Chemical Engineering and Petroleum Processing (CEPP), Ho Chi Minh City University of Technology – Vietnam National University, 268 Ly Thuong Kiet Street, Ward 14, District 10, Ho Chi Minh City, Vietnam

<sup>b</sup>Faculty of Chemical Engineering, Ho Chi Minh City University of Technology - Vietnam National University, 268 Ly Thuong Kiet Street, Ward 14, District 10, Ho Chi Minh City, Vietnam

<sup>c</sup>Key Laboratory of Applied Physical Chemistry, University of Science - Vietnam National University, 227 Nguyen Van Cu Street, Ward 4, District 5, Ho Chi Minh City, Vietnam  
 nhhieubk@hcmut.edu.vn

In this study, graphene oxide (GO) was synthesized using the improved Hummers' method, and reduced graphene oxide (rGO) was synthesized from GO with hydrazine hydrate as reducing agent. Zinc oxide (ZnO) was synthesized from zinc acetate using the precipitation method. Zinc oxide/reduced graphene oxide (ZnO/rGO) composites were synthesized using the ex-situ method. The ZnO/rGO composites with different rGO weight percents (0.05, 0.1, 0.5, 1, and 5 wt%) were used for fabrication of ZnO/rGO anodes. A control anode was fabricated from ZnO (ZnO anode). The band gaps of fabricated anodes were measured using the ultraviolet–visible spectroscopy (UV-vis). The dye-sensitized solar cells (DSSCs) were assembled and investigated by current density–voltage (J-V) curves and electrochemical impedance spectroscopy (EIS). The ZnO/rGO composite with appropriate rGO content was determined to be 1 wt%, with the efficiency of 1.55 %. The Fourier-transform infrared spectroscopy (FTIR), Raman spectroscopy, X-ray diffraction (XRD) results confirmed wurzite structure of ZnO and the reduction of functional groups of GO to create rGO and ZnO/rGO. The transmission electron microscopy (TEM) showed that the ZnO nanoparticles with size of 10 – 20 nm were evenly distributed on rGO sheets. These results indicated that ZnO/rGO could be the potential material to improve the efficiency of DSSCs.

### 1. Introduction

Nowadays, the alternative to implement a clean energy sources or renewable energy is necessary for the sustainable development. The dye-sensitized solar cells (DSSCs), which are the third generation of solar cells, has attracted attention from researchers due to its simple fabrication procedures, environmental friendliness, and good plasticity (Singh and Nalwa, 2015). DSSCs consist of four components: anode, dye-sensitizer, electrolyte solution, and cathode. In the structure of DSSCs, the anodes are fabricated from titanium dioxide (TiO<sub>2</sub>) or zinc oxide (ZnO). Recently, graphene has been studied to synthesis the composite material for enhancement of DSSCs efficiency (Roy-Mayhew and Aksay, 2014). Graphene is a promising one-atom-thickness material with sp<sup>2</sup>-hybridized carbon atoms packed into a hexagon structure. Graphene has extremely large surface area, high conductivity, high carrier mobility, and chemical inertness (He et al, 2017). Among the synthesis routes of graphene, reduction of graphene oxide (GO) is an efficient, low-cost, and simple method. GO is a material contains functional groups on the carbon hexagon lattice structure. By a controlled reduction procedure, the structural changes from GO to reduced graphene oxide (rGO) with similar structure to graphene (Singh and Nalwa, 2015).

The existence of electron recombination in the ZnO anodes was a phenomenon that decreased the DSSCs efficiency. Therefore, graphene was incorporated with ZnO in order to reduce the electron recombination process of anodes (Cisnerosa et al., 2014). This paper focused on determining the appropriate weight percent

of ZnO in ZnO/rGO3 that can be applied in anode for DSSC assembly to enhance the efficiency (Bykkam et al., 2017). Besides, in this study, the screen-printing method was used for fabrication of anodes in DSSCs. This method was simple and suitable for industrial large-scale production.

In this study, zinc oxide/reduced graphene oxide (ZnO/rGO) composite materials were fabricated by in-situ method with 4 different weight percent of rGO: 0.1, 0.5, 1, and 5 wt%. Then, ZnO/rGO composites were coated on fluorine doped tin oxide (FTO) substrate to fabricate the ZnO/rGO anodes in DSSCs using the screen printing technology. The performances of DSSCs were measured by current density-voltage (J-V) curves and electrochemical impedance spectroscopy (EIS). The ZnO/rGO composite with the highest efficiency was selected for characterization using the Fourier-transform infrared spectroscopy (FTIR), Raman spectroscopy, X-ray diffraction (XRD), and transmission electron microscopy (TEM).

## 2. Materials and methods

### 2.1 Materials

Sulfuric acid (98 %), phosphoric acid (85 %), hydrogen peroxide (30 %), and hydrazine hydrate (99 %) were purchased from Xilong Scientific (China).  $\gamma$ -butyrolacton (GBL) (99 %), ethyl cellulose (99 %), and  $\alpha$ -terpineol (99 %) were purchased from Sigma-Aldrich (Germany). High stability electrolyte (HSE), Surlyn, Platinum Conductor Paste (commercial Pt paste), and fluorine-doped tin oxide (FTO) were purchased from Dyesol (Australia). Acetonitrile (99 %) and graphite were purchased from Sigma-Aldrich (Germany). Potassium permanganate (99 %) and ethanol (99 %) was purchased from Duc Giang Chemical JSC (Vietnam).

### 2.2 Synthesis of GO, rGO, ZnO, and ZnO/rGO composites

GO was synthesized from Graphite (Gi) using the improved Hummers' method (Marcano et al., 2010). 0.1 g of obtained GO was dispersed in 100 mL of H<sub>2</sub>O under ultrasonic for 45 min. 3 mL of hydrazine hydrate was added to the mixture and heated at 70 °C for 2 h. The mixture was sublimated for 12 h to obtain rGO.

ZnO/rGO composites were synthesized using the in-situ method (Bykkamat et al., 2017). GO was dispersed in 2 mL of isopropanol and ZnC<sub>4</sub>H<sub>6</sub>O<sub>4</sub>·2H<sub>2</sub>O under ultrasonic for 30 min. The rGO weight percents of composites were 0.1, 0.5, 1, and 5 %, the sample were marked as ZnO/rGO1, ZnO/rGO2, ZnO/rGO3, and ZnO/rGO4. KOH was sequentially added to the mixture. After continuous stirring for 2 h, the white precipitation appeared in the mixture. Then, hydrazine hydrate was added and the mixture was stirred for 2 h at 70 °C. The mixtures were heated at 450 °C for 4 h to obtain ZnO/rGO composite materials. ZnO powder was synthesized with the same process, without the amount of GO. Band gap energy values of ZnO/rGO and ZnO were determined using the UV-Vis spectrophotometer (Jasco V-670, Germany) with the wavelength of 200 – 800 nm.

### 2.3 Fabrication of anodes and DSSCs assembly

ZnO/rGO or ZnO powders were dispersed in 2 mL of absolute ethanol under ultrasonic for 30 min. ZnO/rGO, or ZnO powder was dispersed in 2 mL of absolute ethanol under ultrasonic for 30 min. Mixture of 128 mg of GBL, 1,600 mg of  $\alpha$ -terpineol, and 2,400 mg of ethyl cellulose were added. The ethanol solvent was evaporated at 45 °C, 70 mmHg for 90 min to obtain the ZnO/rGO or ZnO pastes.

FTO substrates were coated with ZnO/rGO, ZnO pastes using the screen printing technology. After each coating, the electrode was dried at 120 °C for 15 min and then heated at 550 °C for 30 min. The electrodes soaked in the N719 solution to obtain anodes. The fabricated anodes were marked as ZnO, ZnO/rGO1, ZnO/rGO2, ZnO/rGO3, and ZnO/rGO4, corresponding to the composite pastes (0.1, 0.5, 1, and 5 %). The DSSCs were marked as ZnO, ZnO/rGO1, ZnO/rGO2, ZnO/rGO3, and ZnO/rGO4, corresponding to the assembled anodes. FTO substrate was coated with commercial Pt paste to fabricate cathode. The electrode was dried at 120 °C for 15 min and heated at 450 °C for 30 min to obtain cathode.

Assembling of cathodes and anodes was conducted in the glove box with nitrogen environment. The electrodes were fitted and bonded together by Surlyn. After that, HSE electrolyte was injected into cells. Subsequently, the cells were pressed by heat press machine at 170 °C for 15 s to obtain final DSSCs.

The J-V curve measurement was performed under simulated light at 750 W/m<sup>2</sup> with a solar simulator (HMT Co., India) using the Keithley 2400 potentiostat (Keithley Instruments Inc., USA). The values of short circuit current density ( $J_{sc}$ ), open circuit voltage ( $V_{oc}$ ), fill factor (ff), and efficiency ( $\eta$ ) were displayed from the instrument software. EIS method was used for investigating the electron transfer process in the DSSCs, measured in the dark using the EIS VersaStat3 (Ametek, USA). The appropriate composite material was determined by the highest DSSC efficiency and selected for characterization.

### 2.4 Characterizations

FTIR (Bruker FT-IR Alpha, Germany) was used for detecting the functional groups in the structure of Gi, GO, rGO, and ZnO/rGO; with the DTGS detector. Raman spectroscopy (LabRam HR Evolution, Japan) was

utilized to characterize the properties and disorders in the structure of Gi, GO, rGO, and ZnO/rGO. The exciting wavelength was 632 nm, measured with the Helium and Neon environment. XRD (Bruker D2 Phaser, Germany) was used for determining the gap between layers of GO, rGO, and characteristic diffractions of GO, rGO, ZnO, and ZnO/rGO. The XRD measurements were performed with  $\lambda = 0.154$  nm, SSD160 Lynxeye detector. TEM image (Joel JEM-1400Plus, USA) was applied to investigate of the morphology of appropriate ZnO/rGO material with the maximum accelerating voltage of 120 kV.

### 3. Results and discussions

#### 3.1 Band gap measurement

The UV-vis spectra of ZnO and ZnO/rGO composites were shown in Figure 1. The band gap values of synthesized ZnO and ZnO/rGO were calculated from the absorption spectra. The absorption band at about 380 nm of ZnO or ZnO/rGO patterns could be attributed to the highly crystalline of ZnO structure. The decrease of the absorbance intensity from the absorption peak was due to electron promotion of ZnO from the valence band to the conduction band. As shown in Table 1, the band gap values of ZnO/rGO composites were narrowed, compared with ZnO. Because rGO was incorporated in the structure of ZnO, resulting in the formation of Zn–O–C bonds in the composite and decrease of the band gap energy of ZnO/rGO composites (Philip et al., 2018). The absorption peak and band gap values of ZnO and ZnO/rGO were approximately equal with other materials from previous studies, indicating successful synthesis of ZnO/rGO composites.

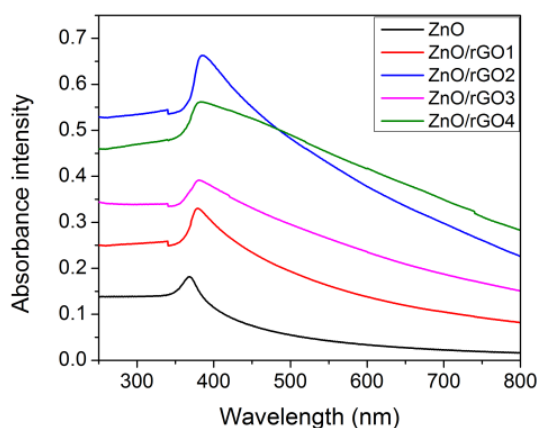


Figure 1: UV-vis spectra of fabricated anodes

Table 1: UV-vis absorption peak and band gap values of ZnO and ZnO/rGO composites

Anodes	rGO weight percent (wt%)	Absorption peaks (nm)	Band gaps (eV)	Refs.
ZnO	0	365	3.05	This study
ZnO/rGO1	0.1	379.5	2.56	This study
ZnO/rGO2	0.5	381.5	2.48	This study
ZnO/rGO3	1	383	2.30	This study
ZnO/rGO4	5	385	1.76	This study
ZnO	0	364	3.00	(Bykkam et al, 2017)
ZnO/rGO	3	~364	2.17	(Bykkam et al, 2017)
ZnO/rGO	0.5	-	3.05	(Siwach et al., 2017)
ZnO/rGO	-	365	2.56	(Philip et al., 2018)

#### 3.2 DSSCs performance

As shown in Figure 2, J-V curves of fabricated DSSCs were measured and the photovoltaic parameters were summarized in Table 2. The fill factor of manufactured DSSCs showed the increase ff values when the rGO wt% was increased. The efficiencies of ZnO/rGO1, ZnO/rGO2, and ZnO/rGO3 DSSCs were 1.25, 1.47, and 1.55 %, which were higher than that of ZnO DSSC (1.08 %). The ff values and efficiency were two important parameters for evaluation of DSSCs. It could be seen that DSSCs efficiency were improved with the presence of rGO. During the injection of excited electron from dye to FTO, the electron–hole recombination could

considerably reduce the efficiency of DSSCs. The addition of rGO, a high conductivity and high electron mobility material, improved the transport pathway of the excited electrons, prevented the electrons – holes recombination, and enhanced the efficiency of DSSC (Bykkam et al., 2017). ZnO/rGO4 DSSC demonstrated a low efficiency, due to the decrease of transmittance of anode. The excessive amount of graphene could become the recombination center that facilitated recombination of electrons (Siwach et al., 2017). The appropriate rGO weight percent in the composite was 1 %, corresponding to the ZnO/rGO3 DSSC, which exhibited the highest efficiency. The efficiencies of fabricated DSSCs were compared with other results from previous studies. The efficiency results in this study were higher than other reports, indicating the successful fabrication of ZnO/rGO for enhancement of DSSCs efficiency.

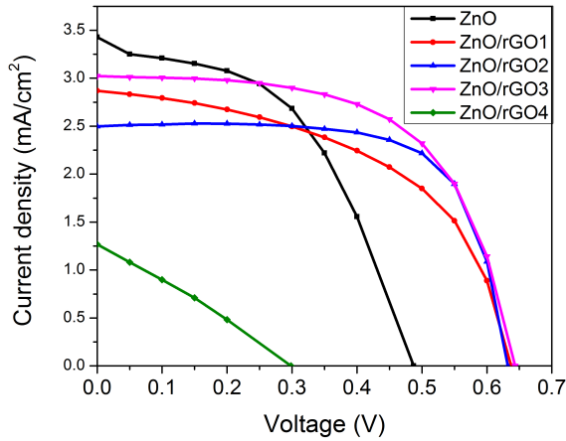


Figure 2: J-V curves of fabricated DSSC

Table 2: Photovoltaic parameters of fabricated DSSCs

DSSC	$V_{oc}$ (V)	$J_{sc}$ (mA.cm <sup>-2</sup> )	ff	$\eta$ (%)	Reference
ZnO	0.48	3.43	0.49	1.08	This study
ZnO/rGO1	0.64	2.87	0.51	1.25	This study
ZnO/rGO2	0.63	2.50	0.70	1.47	This study
ZnO/rGO3	0.64	3.02	0.60	1.55	This study
ZnO/rGO4	0.30	1.27	0.28	0.14	This study
ZnO nanoparticles	0.62	3.99	0.48	1.18	(Li et al., 2013)
ZnO/commercial Gr	0.43	1.93	0.13	0.44	(Philip et al., 2018)
ZnO/rGO	0.53	1.91	-	0.52	(Khurana et al., 2013)

As shown in Figure 3a, the equivalent circuit model [ $R_s(C_{CE}/R_1)(C_{\mu}/R_2)$ ] was applied with the Nyquist plots diagram. There are three semicircles in EIS Nyquist plots of normal DSSC. The first high-frequency semicircle represented the charge transfer on the interface between cathode and electrolyte. The second middle-frequency semicircle represented to electron transfer in the anode. The third low-frequency semicircle, which represented the ions diffusion process in the electrolyte between anode and cathode, was not observed due to the rapid diffusion of the HSE electrolyte in DSSCs (Khurana et al., 2013). Under dark condition, the  $R_2$  value represented the recombination of electrons at the anode/dye/electrolyte interface.

As shown in Figure 3b, The  $R_2$  values of ZnO/rGO1, ZnO/rGO2, and ZnO/rGO3 DSSCs were 931.6, 986.7, and 1029  $\Omega$ , respectively. These results were higher than that of ZnO DSSC (731  $\Omega$ ), indicating the lower of recombination rates in the ZnO/rGO anodes, compared with the ZnO anodes. The incorporation of rGO in the structure of ZnO/rGO composite improved the transport pathway, reduced the recombination of excited electrons, and reduced the transmission resistance between the ZnO, FTO, and electrolyte solution (Mehmood et al., 2015). The  $R_2$  value of ZnO/rGO4 DSSC was 524.5  $\Omega$ , lower than that of ZnO DSSC. When the weight percent of rGO was higher than 1 wt%, the excessive amount of graphene could become the recombination center (Siwach et al., 2017) and hinder the continuous structure of ZnO network (Cai et al., 2017). The J-V and EIS results demonstrated that ZnO/rGO3 was the appropriate composite for fabrication of anode in DSSC with the highest efficiency (1.55 %). ZnO/rGO3 was selected for characterization.

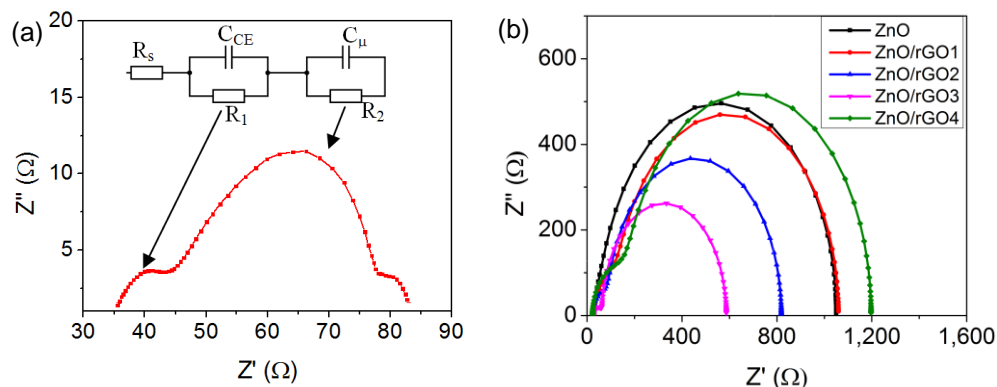


Figure 3: (a) Equivalent circuit model [ $R_s(C_{CE}/R_1)(C_{II}/R_2)$ ] of DSSCs; (b) EIS Nyquist plots of fabricated DSSCs

### 3.3 Characterizations

Figure 4 demonstrates the FTIR and Raman spectra of Gi, GO, rGO, and ZnO/rGO. The FTIR spectrum of GO showed characteristic peaks at 1,236.54, 1,629.26, and 3,397.38  $\text{cm}^{-1}$ , corresponding to the vibrations of the epoxide (C-O-C), carboxylic (C=O), and hydroxyl (-OH) groups (Marcano et al., 2010). These results showed that Gi was oxidized to obtain GO. The characteristic peaks of GO were reduced or disappeared on the spectra of GO and ZnO/rGO, indicating that the functional group of GO was reduced to create rGO and ZnO/rGO (Marcano et al., 2010). The FTIR spectrum of ZnO/rGO3 demonstrated two peaks at 507.14 and 433.23  $\text{cm}^{-1}$ , corresponding to the Zn-O vibration of hexagonal wurtzite structure (Philip et al., 2018).

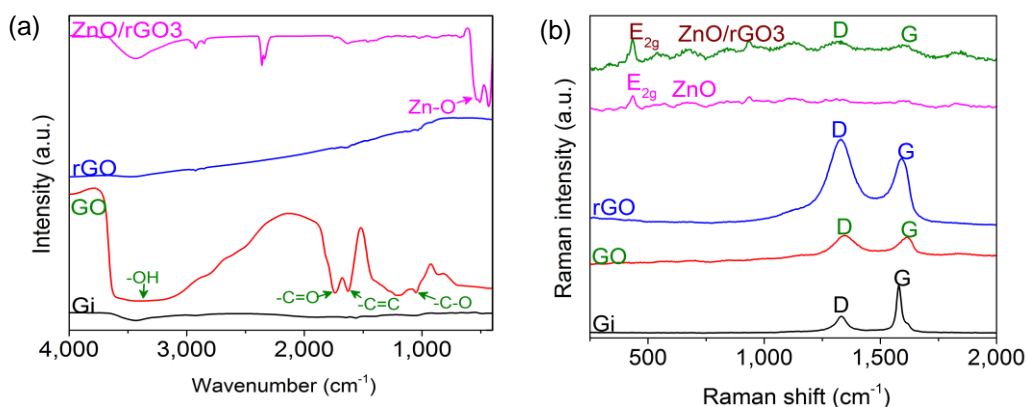


Figure 4: (a) FTIR spectra and (b) Raman spectra of Gi, GO, rGO, ZnO, and ZnO/rGO3

Raman spectra of Gi, GO, rGO, and ZnO/rGO3 had two peaks: the D-band peak at low wavenumber and G-band peak at higher wavenumber. The ratio of D-band to G-band ( $I_D/I_G$ ) is usually used for evaluating the disorder of carbon networks. The  $I_D/I_G$  ratio of GO and Gi exhibited the increase of disorder in the structure of GO, compared with Gi. Because the synthesis of GO increased the disorder in the hexagonal structure and  $sp^3$  hybridizations (Bykkam et al., 2017). In the Raman spectra of ZnO and ZnO/rGO3, the vibration peak at 436  $\text{cm}^{-1}$  was assigned to the  $E_2$  non-polar phonon modes, corresponding to the hexagonal crystal structure of ZnO nanoparticles. The D-band and G-band peaks of ZnO/rGO3 spectrum were unclear, due to the low amount of rGO in the structure of ZnO/rGO3 (Khurana et al., 2013).

The XRD patterns of GO, rGO, and ZnO/rGO3 materials are demonstrated in Figure 5a. The (002) peak of rGO was shifted from  $2\theta = 13.68^\circ$  to  $25.06^\circ$ , similar to Gi and the interlayer distance between the rGO was determined to be 0.35 nm. The interlayer distance of rGO was reduced because most of the oxygen-containing functional groups were removed after reduction process. The diffraction peaks of ZnO/rGO3 were appeared at  $2\theta = 31.8^\circ$ ;  $34.5^\circ$ ;  $36.3^\circ$ ;  $47.5^\circ$ ;  $56.6^\circ$ ;  $62.8^\circ$ ;  $67.9^\circ$ , and  $69.0^\circ$ , corresponding to the (110), (002), (101), (102), (110), (103), (112), and (201) plane; matched with the JCPDS File No.36-1451 for wurtzite structures (Bykkam et al., 2017). The diffraction peaks of GO, rGO were not observed in the XRD pattern of ZnO/rGO3, because the weight percent of rGO in ZnO/rGO3 composite was very low (1 %).

As shown in Figure 5b, the TEM images of the ZnO/rGO3 demonstrated the decoration of ZnO nanoparticles on rGO sheets. The ZnO nanoparticles with average size of 10 nm were evenly distributed on rGO, which was observed to be the semi-transparent thin layer, indicating that the 2D structure of rGO were maintained. These results exhibited the good incorporation of rGO sheets and ZnO nanoparticles in the structure of ZnO/rGO3.

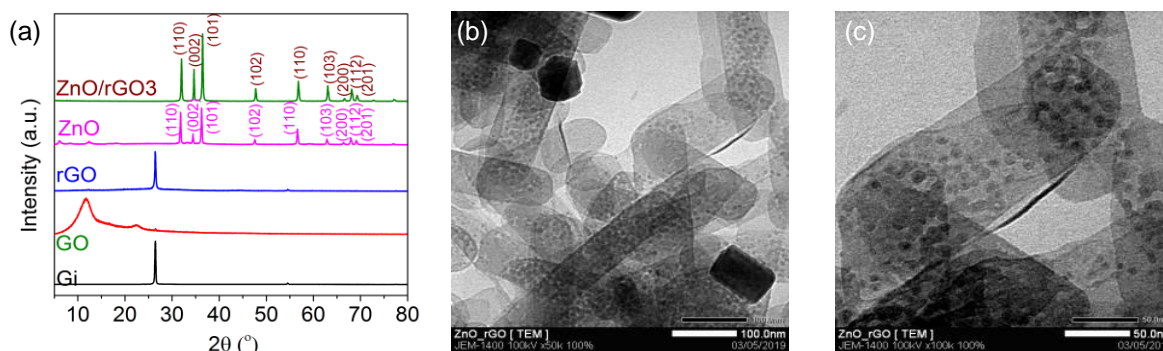


Figure 5: (a) XRD patterns of synthesized materials; TEM images of ZnO/rGO3 at (b) 100 nm and (c) 50 nm

#### 4. Conclusion

In this study, the ZnO/rGO composite was synthesized using the in-situ method, with hydrazine hydrate as reducing agent. The appropriate composite material is ZnO/rGO3 with the rGO percent of 1 %. The efficiency of DSSC fabricated from ZnO3/rGO was higher than that of ZnO. Characterizations of appropriate composite material demonstrated that the ZnO was decorated on rGO sheets, with the diameter of 10 – 20 nm. These results have shown the possibility of incorporation of rGO to fabricate anode of DSSC.

#### Acknowledgment

This research was financially supported by Ho Chi Minh City Department of Science and Technology in 2019.

#### References

- Bykkam S., Kalagadda V. R., Kalagadda B., Selvam K. P., Hayashi, Y., 2017, Ultrasonic-assisted synthesis of ZnO nano particles decked with few layered graphene nanocomposite as photoanode in dye-sensitized solar cell, *Journal of Materials Science: Materials in Electronics*, 28, 6217-6225.
- Cai H., Li J., Xu X., Tang H., Luo J., Binnemans K., Fransaer J., De Vos D.E., 2017, Nanostructured composites of one-dimensional TiO<sub>2</sub> and reduced graphene oxide for, *Journal of Alloys and Compounds*, 697, 132-137.
- Cisnerosa R., Beleyb M., Lopicque F., 2014, Electrochemical impedance model of a (low-cost) dye-sensitized solar cell, *Chemical Engineering Transactions*, 41, 193-198.
- He Q., 2017, Application of the graphene/ZnO composites in treatment of the simulated ceftazidime wastewater. *Chemical Engineering Transactions*, 62, 109-114.
- Khurana G., Sahoo S., Barik S. K., Katiyar R. S., 2013, Improved photovoltaic performance of dye sensitized solar cell using ZnO-graphene nano-composites, *Journal of Alloys and Compounds*, 578, 257-260.
- Li H., Bai J., Feng B., Lu X., Weng J., Jiang C., Wang J., 2013, Dye-sensitized solar cells with a tri-layer ZnO photo-electrode, *Journal of Alloys and Compounds*, 578, 507-511.
- Marcano D.C., Kosynkin D.V., Berlin J. M., Sinitiskii A., Sun Z., Slesarev A., Alemany L. B., Lu W., Tour J. M., 2010, Improved synthesis of graphene oxide, *American Chemical Society Nano*, 4, 4806-4814.
- Mehmood U., Ahmed S., Hussein I. A., Harrabi, K., 2015, Improving the efficiency of dye sensitized solar cells by TiO<sub>2</sub>-graphene nanocomposite photoanode, *Photonics and Nanostructures-Fundamentals and Applications*, 16, 34-42.
- Philip M.R., Nguyen H., Babu R., Krishnakumar V., Bui T.H., 2018, Polyol synthesis of zinc oxide-graphene composites: Enhanced dye-sensitized solar cell efficiency, *Current Nanomaterials*, 3, 52-60.
- Roy-Mayhew J.D., Aksay I.A., 2014, Graphene materials and their use in dye-sensitized solar cells, *Chemical reviews*, 114, 6323-6348.
- Singh E., Nalwa H.S., 2015, Graphene-based dye-sensitized solar cells: A review, *Science of Advanced Materials*, 7, 1863-1912.
- Siwach B., Mohan D., Jyoti D., 2017, To investigate opulence of graphene in ZnO/graphene nanocomposites based dye sensitized solar cells, *Journal of Materials Science: Materials in Electronics*, 28, 11500-11508.